Internal Transport Barrier Triggered by Neoclassical Transport in W7-AS

U. Stroth,[2] K. Itoh,[3] S.-I. Itoh,[4] H. Hartfuss,[1] H. Laqua,[1] the ECRH team,[1] and the W7-AS team[1]

[1]*Max-Planck-Institut für Plasmaphysik, EURATOM Association, D-85748 Garching, Germany*
[2]*Institut für Experimentelle und Angewandte Physik, CAU Kiel, 24098 Kiel, Germany*
[3]*National Institute for Fusion Science, 322-6 Oroshi, Toki, Gifu 509-5292, Japan*
[4]*Kyushu University, Kasuga 816-8580, Japan*

(Received 23 October 2000)

The three-dimensional magnetic configuration of a stellarator offers two specific mechanisms for a transition to improved particle and energy confinement. One route goes through the so-called electron-root confinement regime, which leads to a reduction of neoclassical transport via strong radial electric fields. In this Letter evidence for a second route is presented. It opens due to the layer of a strongly varying radial electric field which is present in the transitional region from neoclassical electron to ion-root confinement. This type of improvement acts on turbulent transport.

DOI: 10.1103/PhysRevLett.86.5910 PACS numbers: 52.55.Hc, 52.25.Fi

Transport of energy and particles in magnetically confined high-temperature plasmas is in general strongly enhanced above the neoclassical transport, i.e., the collisional flux-level estimates. The enhancement is attributed to turbulence, and this is independent of the specific magnetic configuration. Systems with toroidal symmetry, such as tokamaks, show the same level of transport as devices without this symmetry, such as helical systems [1,2]. For the construction of a fusion power reactor, a transport reduction with respect to the so-called *L*-mode confinement level is needed. The most efficient reductions achieved are by transport barriers such as the *H* mode [3] or the internal transport barriers [4]. It is generally accepted that the turbulence reduction is due to a sheared $\mathbf{E} \times \mathbf{B}$ flow generated by a radially varying radial electric field (see, for a review, [5,6]).

The three-dimensional magnetic field configuration of stellarators bears an additional loss channel for particles and energy. It opens due to the collisionless loss of particles trapped in local magnetic mirrors. The related particle fluxes are nonambipolar and hence they create a radial electric current to modify the radial electric field. This electric field generation opens two stellarator-specific routes to transport reduction.

Generally, in both cases a plasma with strongly heated electrons is needed to make electron losses superior to ion losses. In the plasma center, the plasma potential turns from negative or small positive to strongly positive values. This features is called the electron root (ER) and has been observed in CHS [7,8] and in W7-AS [9,10] right in the plasma core. The electron root is characterized by a strong reduction of neoclassical transport within the region where a strong positive electric field exists. The neoclassical diffusivity drops to values of the order of 0.1 m^2/s. As illustrated in Fig. 1, an additional potential for transport reduction occurs at the transition layer from the electron-root to the ion-root (IR) regime. In this region the potential changes from strongly positive to small or negative values. It therefore consists of a layer with strongly sheared plasma flow, which is able to reduce turbulent transport. Accordingly, a strong inhomogeneity of the radial electric field at the interface between positive and negative electric fields has been observed in CHS. A consecutive increase of the central electron temperature has been observed as well [8]. However, the structure and transition characteristics of the energy transport barrier have not been studied.

This Letter reports on first experimental evidence of such a transport barrier in the transition layer between the two neoclassical regimes, and it describes the associated structure and hysteresis properties found in the electron energy transport channel.

The two possible mechanisms of transport reduction can be distinguished by the following signatures (see Fig. 1 for illustration): (i) The electron root reduces the neoclassical contribution to the total transport to very small values everywhere in the region with a radial electric field $E_r \gg 0$. The turbulent transport is only weakly affected by the magnitude of the electric field, and hence the experimental diffusion coefficient should be on the level of turbulent transport, which is in the *L* mode for the investigated parameters typically ≥ 1 m^2/s—well above the neoclassical value in the ER regime.

(ii) The shear layer in the transition region from the ER to the IR regime has the potential to strongly stabilize the turbulence and reduce the total diffusivity to the level of neoclassical transport. Since in the present investigation this shear layer coexists with the ER regime, the neoclassical level in this region is also very low. Therefore, a turbulence suppression in the radially limited shear layer will lead to a transport barrier with a strong increase of the temperature gradient. The structure of transport barriers has been discussed in [11–13]. (iii) The development of a transport barrier depends in a nonlocal way on plasma parameters, therefore a hysteresis both in electron temperature T_e and heating power P should appear [14].

To investigate these signatures, two types of discharges were analyzed. The radial region of transport reduction is investigated on plasma discharges with a sequence of

 0031-9007/01/86(26)/5910(4)$15.00

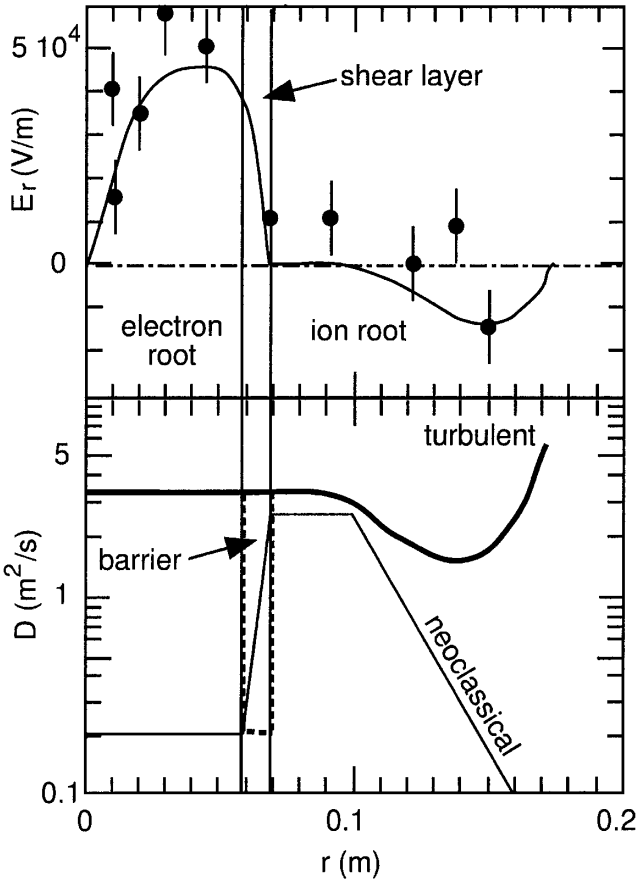

FIG. 1. Sketch of two stellarator-specific mechanisms reducing transport. Top: Radial electric field with a transition from the neoclassical electron-root (ER) into the ion-root (IR) regime. Bottom: The turbulent and neoclassical transport (calculated with the field from the top) contributions and a transport barrier in the E_r shear layer. The shown values are characteristic for low density ECH discharges when the electron root develops. The data points are taken from [10].

forth and back transitions. Hysteresis effects are studied on recent discharges where the heating power was varied continuously.

The transport coefficients shown in Fig. 1 are calculated for the improved confinement phase of the discharge from Fig. 2. The diffusivities are calculated as power flux divided by measured temperature gradient. The neoclassical flux is calculated from the DKES code and the experimental one is equal to the heating power. For clarity, the profile shapes were simplified within the error bars. All neoclassical quantities are from a self-consistent calculation fitting the experimental density and temperature profiles. The electric field data shown in Fig. 1 are from a stationary state of a discharge similar to the discharges analyzed here [9,10].

Figure 2 depicts time traces of the electron cyclotron emission (ECE) electron temperature from a W7-AS discharge undergoing several pronounced forth and back transitions into improved core confinement. The temperature increases by 0.7 keV to about 4.8 keV. The line average density was $\bar{n}_e = 3.5 \times 10^{19}$ m^{-3}, the magnetic field

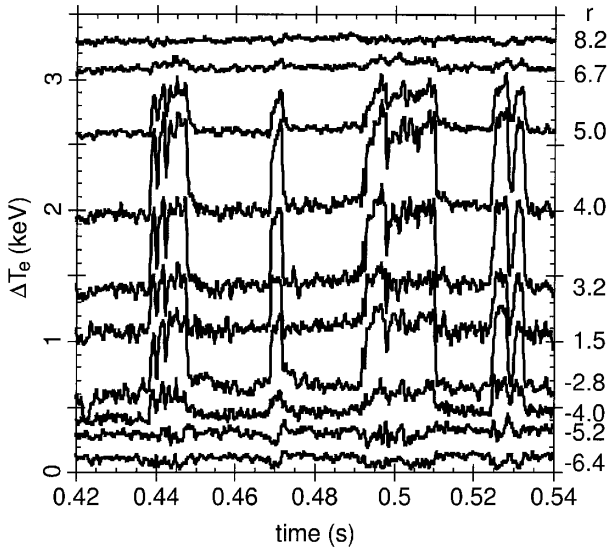

FIG. 2. ECE measurements of the electron temperature in discharge No. 42975 with multiple transitions low and improved confinement. The individual traces are shifted by arbitrary values. On the right, the radial location of the measurements in centimeters is shown.

strength $B = 2.5$ T, the rotational transform $\iota = 0.34$, and the heating power $P = 1.27$ MW. The presented phase of the discharge has parameters sufficient to access the neoclassical electron-root regime; details can be found in [9,10]. Figure 2 depicts the temporal electron temperature changes at various radii. Negative radii indicate the high-field side of the plasma. For better visibility the time traces were shifted by arbitrary values. It can be seen that the modification of the electron temperature due to the transitions is concentrated to the plasma core with an effective radius of $|r| \leq 6$ cm. The asymmetry between the high- and the low-field side is due to imperfect correction of the Shafranov shift. The increase of the electron temperature is almost the same on the four innermost channels. This indicates that the improvement is due to a localized transport barrier.

In Fig. 3, the change of the temperature gradient is explored. These time traces were obtained by taking the differences of adjacent channels and dividing them by the radial separation. Again, the time traces are shifted by arbitrary numbers. Because of the Shafranov shift, one has to symmetrize to obtain the radial information. Since radiative losses and ion-electron coupling are negligible in the core, the time traces are closely related to the thermal diffusivity. The increment of dT_e/dr amounts up to 0.4 keV/cm, which is approximately twice the gradient in the low confinement regime. Absolute values for the electron heat diffusivity (total energy flux divided by temperature gradient) deduced from adjacent ECE channels at $r \approx 4$ cm during the improved phase are in the range of 0.2 m^2/s, and the reduction is of the order of 50%. It is found that the increment of the temperature gradient is localized near the surface around $r \approx 4$ cm. The full width of the layer in which dT_e/dr increases is about 3 cm. This

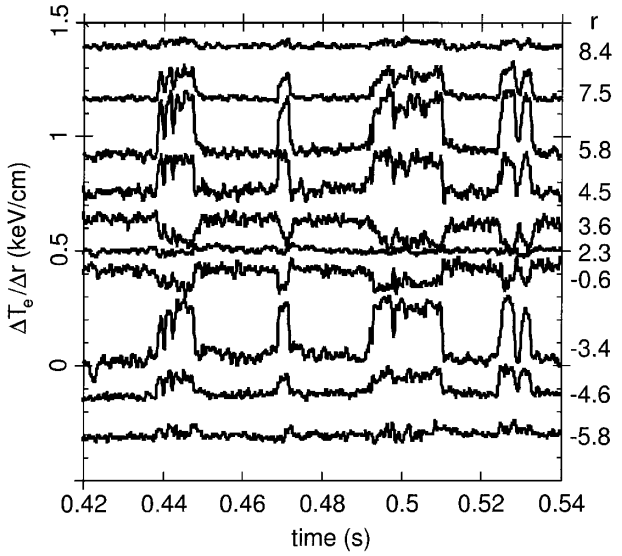

FIG. 3. Change of electron temperature gradient estimated from the time traces of discharge No. 42975 shown in Fig. 2. The individual traces are shifted by arbitrary values.

implies that the reduction is transport, which drives the incremental jump of the central electron temperature, is restricted to a narrow layer around $r \approx 4$ cm. For the inner channels, rather a decrease of the gradient than an increase is observed.

Theoretical neoclassical estimates using the DKES code [15,16] yield that the discharge should transit into the electron-root regime already at an electron temperature of 2 keV. Hence the depicted phase should be deeply in the ER state, and transitions seen at 4 keV are not consistent with a neoclassical prediction for the access of the ER state. The radial region of ER confinement is predicted to be inside 6 cm. This would lead to a shear layer at about 6 cm and would be consistent with the interpretation that confinement improvement is due to a transport barrier in the neoclassically generated shear layer. Furthermore, the observation of a diffusivity well below 1 m^2/s shows that turbulent transport is strongly suppressed. As a third point in favor of a transport barrier, the hysteresis behavior of the transition is discussed below.

A consistent picture emerges as follows: The phase of the discharge shown in Figs. 2 and 3 is in the ER state throughout. Therefore, already prior to the transitions the shear layer can have a reducing impact on turbulence. This explains the low value of $\chi_e \approx 0.5$ m^2/s in the low confinement phase. The jump in electron temperature can then be attributed to the development of a transport barrier, where the sheared flow stabilizes the turbulence. The responsible radial electric field is mainly provided by the neoclassical particle flux. However, contributions from self-generated zonal flow or from nonthermal electrons generated by the intense ECRH cannot be ruled out and might be responsible for the spontaneous transitions.

Turbulence suppression by sheared $\mathbf{E} \times \mathbf{B}$ flow can be expected when the shearing rate exceeds the turbulence growth rate [17]. From Fig. 1 an estimate for the low-magnetic shear plasma is about 1.2×10^6 s^{-1}. This is large compared with typical shearing rates inside tokamak transport barriers and also compared with simple estimates for growth rates of drift waves ($c_s/R \approx 3 \times 10^5$ s^{-1} [18]). Linear growth rates in a stellarator were estimated to be $c_s/3R$ [19].

The bifurcation behavior of the transport barrier was investigated by power-ramp experiments. The plasma parameters were $B = 2.5$ T, $\bar{n}_e = 1 \times 10^{19}$ m^{-3}, and $\iota \approx 1/3$. The power was ramped down from 0.7 to 0.3 MW and ramped back up again (see upper trace in Fig. 4). Figure 4 shows the resulting time traces of the electron temperature at three inner radii. The discharge in the time frame of Fig. 4 starts in the improved regime. In these discharges, an effect of transport reduction is observed only at $r \leq 3$ cm. This might be due to the reduced available power of 0.7 MW.

At 0.62 s the back transition into the low confinement occurs at a heating power of 0.34 MW. The temperatures at the three radii are 3.4, 2.8, and 2.4 keV, respectively. Because of the back transition, the temperature difference between $r = 2$ cm and $r = 3$ cm drops by more than 60%, and that between $r = 0.5$ cm and $r = 2$ cm by more than 50%. This reduction in the gradient reflects the strong increase of total transport at the back transition. After increasing the power again, the transition into improved confinement is observed at a heating power of 0.5 MW and temperatures of 3.8, 3.2, and 3.0 keV. Hence the data show a hysteresis in both temperature and heating power. After the transition into the improved state, the temperature difference between $r = 2$ cm and $r = 3$ cm increases by a factor of 2 and is the same as between $r = 0.5$ cm and $r = 2$ cm. This indicates the reduction of the energy transport coefficient by about a factor of 2. These prominent jumps of the transport coefficient (which is dominated by

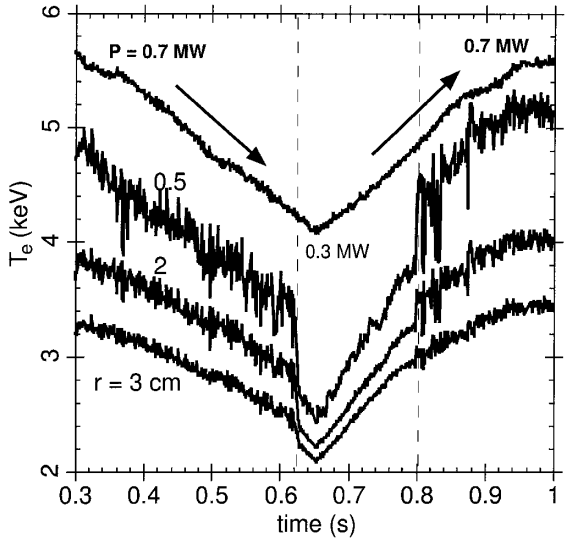

FIG. 4. Heating power (top curve) and three channels (radii in centimeters are indicated) of the ECE electron temperature diagnostics in the power-ramp discharge No. 46388.

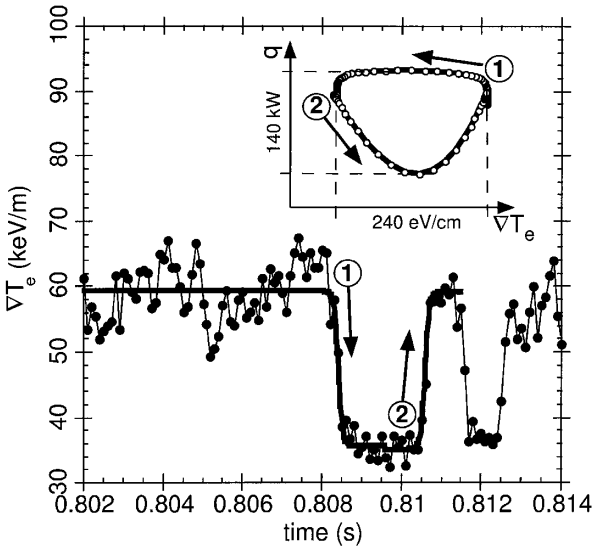

FIG. 5. The temperature gradient of the dithering phase shown in Fig. 4 calculated from the time traces for $r = 0.5$ and 3 cm. A one cycle fit is also shown (solid line). The inset shows from the fit the calculated hysteresis of power flux vs temperature gradient during the cycle. The distance in the time steps of the inset is 0.02 ms.

anomalous transport) at both transitions clearly illustrate the existence of the transport barrier for the electron energy. According to neoclassical calculations, the back transition to the IR regime is expected at $T_e < 200$ eV. This again indicates that the sudden confinement improvement is due to a suppression of turbulent transport in a region which might be preconditioned by neoclassical transport.

In the transition to the improved state ($t = 0.8-0.84$ sec), i.e., near the threshold condition, dithering cycles are observed. In Fig. 5, one of these cycles is analyzed in view of the hysteresis. To this end, the temperature data at $r = 0.5$ and 3 cm from Fig. 4 were used to calculate temperature gradient and average temperature. Both time traces were fitted to calculate the dependence of power flux on temperature gradient as plotted in the inset of Fig. 5. The power flux is the central heating power corrected due to the temporal change of the energy content, $P - dW/dt$, which is calculated from the mean of the two fitted channels multiplied by the plasma volume inside $r = 3$ cm. Data and fit of the temperature gradient are also depicted. The arrows indicate the course of time for the transition to low confinement (1) and back to improved confinement (2). The dots in the inset mark time points every 20 μs. The swing of the hysteresis in power flux is about 140 kW. This behavior shows again that it is not a smooth transition to improved confinement but rather the development of a barrier which can suddenly appear and vanish.

In conclusion, several observations indicate that the confinement improvement observed in strongly ECR heated plasmas is due to the development of an internal transport barrier rather than due to a reduction of neoclassical transport in the electron-root regime. The low value of the diffusivity points to a suppression of turbulent transport, the transport reduction appears in a narrow radial region, and the forth and back transitions as well as the dithering phase prior to the transition exhibit a hysteresis in temperature and heating power at temperature inconsistent with the neoclassical prediction for the ER transition. The reported transition is observed in discharges which have an electron-root core. Therefore, it can be conjectured that it is related to the flow shear layer in between the neoclassical electron- and ion-root regimes. The observed spontaneous transitions might be triggered by self-generated zonal flows inside the layer preconditioned by neoclassical transport. The observed shearing rates are large compared with simple estimates for the turbulence growth rates.

This leads to a stabilization of turbulence and a reduction of turbulent transport in a narrow layer. The transport barrier should also show up as a reduction of the fluctuation level, and it can be argued that the fluctuation reductions observed during the *electric pulsation* in the CHS heliotron [8] are due to a neoclassically driven transport barrier as reported here. Direct observations of the dynamics of E_r and of the turbulence behavior during the oscillations in Fig. 2 are left for future work.

Two of the authors (K. I. and S.-I. I.) acknowledge hospitality of Alexander von Humbolddt Stiftung and Max-Planck-Institut fur Plasmaphysik.

[1] F. Wagner and U. Stroth, Plasma Phys. Controlled Fusion **35**, 1321 (1993).
[2] U. Stroth, Plasma Phys. Controlled Fusion **40**, 9 (1998).
[3] F. Wagner *et al.,* Phys. Rev. Lett. **49**, 1408 (1982).
[4] E. J. Strait *et al.,* Phys. Rev. Lett. **75**, 4421 (1995).
[5] K. Itoh and S.-I. Itoh, Plasma Phys. Controlled Fusion **38**, 1 (1996).
[6] K. H. Burrell *et al.,* Plasma Phys. **4**, 1499 (1997).
[7] H. Idei *et al.,* Phys. Rev. Lett. **71**, 2220 (1993).
[8] A. Fujisawa *et al.,* Phys. Rev. Lett. **82**, 2669 (1999).
[9] M. Kick *et al.,* Plasma Phys. Controlled Fusion **41**, A549 (1999).
[10] H. Maassberg *et al.,* Phys. Plasmas **7**, 295 (2000).
[11] P. H. Diamond *et al.,* Plasma Phys. **2**, 3685 (1995).
[12] P. H. Diamond *et al.,* Phys. Rev. Lett. **78**, 1472 (1997).
[13] K. Itoh, S.-I. Itoh, and A. Fukuyama, *Transport and Structural Formation in Plasmas* (IOP, London, England, 1999), Chap. 12.
[14] S.-I. Itoh and K. Itoh, Phys. Rev. Lett. **60**, 2276 (1988).
[15] W. I. van Rij and S. P. Hirshman, Phys. Fluids B **1**, 563 (1989).
[16] H. Maaßberg *et al.,* Plasma Phys. Controlled Fusion **35**, B319 (1993).
[17] T. S. Hahm and K. H. Burrell, Phys. Fluids **2**, 1648 (1995).
[18] J. W. Connor and H. R. Wilson, Plasma Phys. Controlled Fusion **42**, R1 (2000).
[19] A. Kendl and H. Wobig, Phys. Fluids **6**, 4714 (1999).